Palaeogeography, Palaeoclimatology, Palaeoecology 299 (2011) 83–96

Contents lists available at ScienceDirect

Palaeogeography, Palaeoclimatology, Palaeoecology

journal homepage: www.elsevier.com/locate/palaeo

Comparison of carbonate C and O stable isotope records across the Jurassic/Cretaceous boundary in the Tethyan and Boreal Realms

Karel Žák [a,*], Martin Košťák [b], Otakar Man [a], Victor A. Zakharov [c], Mikhail A. Rogov [c], Petr Pruner [a], Jan Rohovec [a], Oksana S. Dzyuba [d], Martin Mazuch [b]

[a] Institute of Geology AS CR, v.v.i., Rozvojová 269, 165 00 Praha 6, Czech Republic
[b] Institute of Geology and Paleontology, Faculty of Science, Charles University in Prague, Albertov 6, 128 43 Praha 2, Czech Republic
[c] Geological Institute of RAS, Pyzhevski 7, 119017 Moscow, Russia
[d] Trofimuk Institute of Petroleum Geology and Geophysics, Siberian Branch of RAS, Acad. Koptyug av., 3, Novosibirsk, 630090, Russia

ARTICLE INFO

Article history:
Received 19 November 2009
Received in revised form 6 August 2010
Accepted 29 October 2010
Available online 4 November 2010

Keywords:
Jurassic
Cretaceous
Boreal/Tethyan correlation
Carbon and oxygen isotopes
Paleomagnetic record
Belemnites

ABSTRACT

Carbon and oxygen stable isotope records were compared for Jurassic/Cretaceous (J/K) boundary sections located in the Tethyan Realm (Brodno, Western Slovakia, and Puerto Escaño, Southern Spain; bulk limestones), and the Boreal Realm (Nordvik Peninsula, Northern Siberia, belemnites). Since a detailed biostratigraphic correlation of these Tethyan and Boreal sections is impossible due to different faunal assemblages, correlation of the isotope records was based on paleomagnetic data. This novel approach can improve our understanding of the synchroneity of individual isotope excursions in sections where detailed biostratigraphic correlation is impossible. No significant excursions in either the carbon or oxygen isotope records to be used for future Boreal/Tethyan correlations were found around the J/K boundary (the upper Tithonian and lower Berriasian; magnetozones M20n to M18n) in the studied sections. At the Nordvik section, where a much longer section (middle Oxfordian–basal Boreal Berriasian) was documented, the transition from the middle Oxfordian to the Kimmeridgian and further to the Volgian is characterized by a decrease in belemnite $\delta^{18}O$ values (from $\delta^{18}O$ values up to +1.6‰ vs. V-PDB in the Oxfordian to values between +0.3 and −0.8‰ in the late Volgian and earliest Boreal Berriasian). This trend, which has previously been reported from the Russian Platform and Tethyan Realm sections, corresponds either to gradual warming or a decrease in seawater $\delta^{18}O$. Supposing that the oxygen isotope compositions of seawater in the Arctic/Boreal and Tethyan Realms were similar, then the differences between oxygen isotope datasets for these records indicate differences in temperature. The Boreal/Tethyan temperature difference of 7–9 °C in the middle and late Oxfordian decreases towards the J/K boundary, indicating a significant decrease in latitudinal climatic gradients during the Late Jurassic. Two positive carbon isotope excursions recorded for the middle Oxfordian and upper Kimmeridgian in the Nordvik section can be correlated with a similar excursion described earlier for the Russian Platform. Minor influence of biofractionation at the carbon isotopes, and the influence of migration of belemnites to deeper, slightly cooler water at the oxygen isotopes, cannot be excluded for the obtained belemnite data.

1. Introduction

Biostratigraphic correlation of Mesozoic strata deposited in the Tethyan and Boreal Realms remains difficult, since the existence of geographical barriers as well as the different climatic and paleoecologic conditions of these regions resulted in different faunal assemblages. Correlation of the Jurassic/Cretaceous boundary (J/K boundary in the text later) between sections located in the Tethys–Panthalassa and Panboreal Superrealms is particularly problematic (Jenkyns et al., 2002; Michalík, 2009; Nikitenko et al., 2008; Wimbledon, 2008; Zakharov and Rogov, 2008a,b).

A possible method to correlate the Tethyan and Boreal sections is the application of magnetostratigraphy. The first Tethyan–Boreal correlation of the J/K boundary interval based on magnetostratigraphy was published by Houša et al. (2007). Details on unequivocal identification of individual magnetozones and subzones in the J/K boundary interval are contained in Houša et al. (1999, 2004, 2007, 2008), Pruner et al. (2007), Schnabl et al. (2008) and Pruner et al. (2010). Following the recommendation by the Subcommission of Cretaceous Stratigraphy of the International Commission on Stratigraphy (workshop held at the Università degli Studi di Milano, Italy, March 2009), the J/K boundary interval lies around the base of magnetozone M18r, albeit the discussed interval is much broader, and other proposals (base of the *Hectoroceras*

* Corresponding author.
E-mail address: zak@gli.cas.cz (K. Žák).

0031-0182/$ – see front matter © 2010 Elsevier B.V. All rights reserved.
doi:10.1016/j.palaeo.2010.10.038

kochi Zone, for example) lie within magnetozone M17r. The most frequently proposed J/K boundary (based on calpionellids — i.e., the acme zone of *Calpionella alpina*) is located just below the M18r, close to the Brodno magnetosubzone M19n.1r (Michalík, 2009). This boundary definition is followed herein as well.

Additional information on the correlation of the J/K boundary interval among sections from different climates and bearing different faunal assemblages can be obtained from the C and O stable isotope compositions of limestones and macrofossils. Unfortunately, insufficient stable isotope data on the J/K boundary interval itself are available to allow a correlation between the Tethyan and Boreal Realms. The published stable isotope records across the J/K boundary usually cover much longer time intervals, with relatively loosely spaced sampling points. In this study, attention is focused on a shorter time interval including the late Tithonian and early Berriasian, just across the J/K boundary lying between the M20n and M18n chrons.

Differences in temperatures and depositional environments of the Tethyan and Boreal Realms can be expected to result in systematically different carbonate $\delta^{18}O$ data (assuming similar seawater $\delta^{18}O$; cf. Ditchfield, 1997). Moreover, minor climatic fluctuations are more likely to be observed at higher latitudes, where their pronounced effects should be expected. Changes in the carbonate carbon isotope composition can reflect similar trends in oceanic carbon cycling if seawater of the Tethyan and Boreal Realms was at least partly mixed and/or reflected similar climatic and paleoceanographic evolution. To test these premises, stable isotope data from the J/K boundary section at Brodno (NW Slovkia, Žilina District) published by Michalík et al. (2009) were supplemented by new stable isotope data from the Puerto Escaño section (Southern Spain, Andalusia, Cordoba Province, close to the town of Carcabuey; biostratigraphy and magnetostratigraphy of the section published by Pruner et al., 2010). For the correlation with the Arctic/Boreal Realm, new detailed C and O stable isotope profiles were obtained for one of the northernmost accessible J/K boundary sections, at the coast of the Nordvik Peninsula (Anabar Bay, Laptev Sea, Northern Siberia, Russia; biostratigraphy and description of the section Zakharov and Rogov, 2008b).

The study was complicated by the fact that the two selected Tethyan sections are dominated by limestone, and belemnites are relatively rare, whereas the Boreal section at Nordvik consists of carbonate-poor clastic rocks with abundant belemnites. When analyzing bulk limestone samples the obtained $\delta^{13}C$ stratigraphy is of higher credibility while $\delta^{18}O$ data may be influenced by diagenesis to a higher degree. In contrast, belemnite rostra (if the selected samples are well screened against diagenetic influence) usually yield reliable $\delta^{18}O$ data, but $\delta^{13}C$ values may be influenced by biofractionation already during the life of the belemnites (see in Section 3). Apart from these difficulties, an attempt was made to correlate the stable isotope stratigraphic records of these three sections. With respect to different faunal assemblages, magnetostratigraphy was selected as a primary correlation tool. The thicknesses of section segments between individual magnetic polarity transitions are influenced by changes in the depositional rate. To overcome this complication, a numerical transformation of the actual section readings in meters to the modeled section ages was performed.

2. Published carbon and oxygen stable isotope data close to the J/K boundary

Carbon and oxygen stable isotope data have been published for numerous sections from the Upper Jurassic and Lower Cretaceous. In the Tethyan Realm and other low to intermediate Northern Hemisphere latitudes (ca. 20 to 50°N at the time of deposition, see Dercourt et al., 2000), stable isotope data for the Upper Jurassic and/or Lower Cretaceous sections are quite abundant (e.g., Amodio et al., 2008; Barskov and Kiyashko, 2000; Bartolini et al., 1996; Bodin et al., 2009; Dromart et al., 2003; Gröcke et al., 2003; Jenkyns, 1996; Louis-Schmid et al., 2007; McArthur et al., 2004, 2007b; Michalík et al., 2009; Nunn and Price, 2010; Nunn et al., 2009; Padden et al., 2002; Podlaha et al., 1998; Price and Rogov, 2009; Price et al., 2000; Rogov and Price, 2010; Ruffell et al., 2002; Tremolada et al., 2006; Veizer et al., 1999; Weissert and Channell, 1989; Weissert and Erba, 2004; Weissert and Lini, 1991; Weissert and Mohr, 1996; Zakharov et al., 2005). A composite Tethyan $\delta^{13}C$ curve and a comparison of the Tethyan Realm with data from the Russian Platform can be found in Price and Rogov (2009). This general $\delta^{13}C$ curve for the Tethyan Realm shows high $\delta^{13}C$ values during the Callovian, middle Oxfordian (also studied in detail by Louis-Schmid et al., 2007) and Kimmeridgian, with a pronounced decrease towards the J/K boundary. The generally high $\delta^{13}C$ values of this curve during the Oxfordian are interrupted by two short but pronounced negative shifts. Unfortunately, the Tethyan sections studied isotopically usually do not include paleomagnetic data. This is why Brodno and Puerto Escaño sections (both with detailed magnetostratigraphic record available, Houša et al. 1996, 1999; Pruner et al. 2010) were selected for the present study.

Another region where C and O isotope studies of Upper Jurassic and/or Lower Cretaceous fossils have been performed is the Russian Platform, located between ~30 and 50°N in this period. This region is important for the Boreal/Tethyan correlation. Price and Rogov (2009) significantly extended the Late Jurassic belemnite C and O isotope data for this region previously published by Podlaha et al. (1998), Riboulleau et al. (1998), Barskov and Kiyashko (2000), Ruffell et al. (2002) and Gröcke et al. (2003). Data covering the upper Callovian, Oxfordian, Kimmeridgian and Volgian show an oscillating but distinct trend, with decreasing carbonate $\delta^{18}O$ values toward younger ages. Supposing constant seawater $\delta^{18}O$ values (i.e., either no or constant-volume polar ice, and well mixed seawater), this trend reflects increasing temperatures within the Late Jurassic. The most positive $\delta^{18}O$ values (corresponding to the lowest temperatures) have been found in the latest Callovian. The belemnite $\delta^{13}C$ curve of Price and Rogov (2009) for the Russian Platform also shows a systematic irregular decrease during the Late Jurassic, with several positive excursions, especially in the upper Callovian to lowermost Oxfordian and Kimmeridgian.

Stable isotope profiles across the J/K boundary from high-latitude areas of the Northern Hemisphere are contained in the papers of Ditchfield (1997), and Price and Mutterlose (2004). Ditchfield (1997) studied the C and O isotope compositions of belemnite rostra in a section covering the Middle Jurassic (Aalenian to Bajocian) to the Lower Cretaceous (lower to middle Valanginian) at Kong Karls Land, Svalbard. During the Middle to Late Mesozoic, the Svalbard area was located at approximately 70°N (an estimate based on maps of Smith et al., 1994). Supposing a seawater oxygen isotopic composition of −1‰ (V-SMOW), isotopic temperatures of 12.7 °C were estimated for the Aalenian to Bajocian, 9.4 °C for the early Bathonian to Kimmeridgian, and 7.7 °C for the Valanginian. The sampling covered a rather long time period, and the interval close to the J/K boundary was not analyzed in detail. Price and Mutterlose (2004) published a belemnite C and O isotope profile across the J/K boundary at the Yatria River, Western Siberia. While the area is presently located at 64 to 65°N, it was located at approximately 60°N in the Late Jurassic/Early Cretaceous. The dominant part of the studied section was in the Ryazanian (~Berriasian), Valanginian, and lower Hauterivian, i.e. in the Early Cretaceous. The oldest belemnites analyzed by Price and Mutterlose (2004) belong to the late *Heteroceras kochi* Zone and are therefore younger than the sample set analyzed in this study from the Boreal/Arctic Nordvik section (see next discussion).

One of the important aspects of these studies on Upper Jurassic and Lower Cretaceous sedimentary sequences at high latitudes is the question of whether polar ice caps existed during some periods. Traditionally, the Jurassic and Cretaceous have been considered as periods of warm global climates, weak climatic zoning, and relatively

warm polar regions (e.g., Hallam, 1993). Based on analyses of $\delta^{18}O$ of phosphate from vertebrate tooth enamel, Lécuyer et al. (2003) supposed that limited polar ice could have occurred during the early part of the middle Oxfordian, but relatively low paleotemperatures derived from the Oxfordian fish enamel of the supposed tropical region strictly contradict the northward expansion of coral reefs during the middle to late Oxfordian and possibly reflect the aftermath of the reorganization of currents at the Middle–Late Jurassic transition and a decrease in the latitudinal temperature gradient. Dromart et al. (2003) considered the possible existence of polar ice during the transition from Middle to Late Jurassic (Callovian/Oxfordian; see also Price, 1999; Barskov and Kiyashko, 2000; Nunn et al., 2009), but this suggestion contradicts the high-latitude distribution of glendonites, which occur there commonly during the Bajocian to early Callovian, but are missing in the late Callovian and Oxfordian (Wierzbowski and Rogov, 2009). Several studies have indicated the possibility of limited polar ice caps during some periods of the Early Cretaceous, especially Valanginian (Ditchfield, 1997; Kaplan, 1978; Kemper, 1987; Price and Mutterlose, 2004; Price et al., 2000), late Hauterivian and Aptian (Kemper, 1987; Rogov and Zakharov, 2010). Other studies (Price and Rogov, 2009) have considered alternative interpretations of positive $\delta^{18}O$ oscillations in the Late Jurassic Boreal and Subtethyan sections, such as variation in such factors as seawater salinity and $\delta^{18}O$ values, water depth preferences of belemnites, or their day/night migrations (cf. Dunca et al., 2006).

3. The preservation of original stable isotope records

For paleoclimatic and paleoceanographic interpretations of C and O isotope data obtained either from bulk carbonate rocks or macrofossils, it is essential that only the material which has not undergone diagenetic or later epigenetic alteration is used. Bulk limestone rocks are generally considered a sedimentary medium prone to diagenetic changes. Since the diagenetic alteration of limestones typically proceeds at low water/rock ratio for carbon, but high water/rock ratio for oxygen, the $\delta^{18}O$ data are generally considered to be more sensitive to these diagenetic changes. During usual diagenetic processes (either involving meteoric water or pore water of marine origin, and proceeding at increasing temperature) the $\delta^{18}O$ values of limestone typically decrease, hence the temperatures calculated for diagenetically altered rocks are usually higher than real depositional temperatures. Temperature estimates based on bulk-rock samples can be therefore viewed only as an upper limit of the real depositional temperature. In contrast, carbon from the original sedimentary precursor can be diagenetically transformed into a limestone rock without significant changes in the $\delta^{13}C$ values (Veizer et al., 1999).

For fine-grained bulk limestones, the effects of late-diagenetic (post-lithification) processes on the stable isotope record can be quantified by the measurement of detailed stable isotope profiles (with a sampling step of several mm) across an individual limestone bed or similar profiles perpendicular to diagenetic veinlets, siliceous nodules, etc. Such isotope profiling can show to what degree the original isotopic record has been altered at bed boundaries, which usually have higher porosity, or along structures where diagenetic and epigenetic fluids were channelized. Analyses of whole-rock–belemnite pairs represent another way to improve the understanding of diagenetic vs. biogenic isotopic controls on individual sample types.

The problem of the preservation of original isotopic signals in belemnite rostra has been widely discussed in the literature (Anderson et al., 1994; Ditchfield, 1997; Gröcke et al., 2003; McArthur et al., 2007a; Milliman, 1974; Podlaha et al., 1998; Rosales et al., 2004; Veizer, 1974; Veizer and Fritz, 1976; Wierzbowski and Joachimski, 2009; etc.). Several approaches have been used to avoid altered samples. A combination of textural microscopy with trace element analysis of the best preserved sample section (based on optical analysis — often with the aid of cathodoluminescence) usually permits to select almost unaltered material. Since the contents of some elements (Fe and Mn) in the diagenetic carbonates are much higher than in primary marine calcite, carbonate chemistry is a useful tool to exclude diagenetically altered samples. Various Fe and Mn content value limits have been applied to exclude altered samples (Anderson et al., 1994; Denison et al., 1994; Ditchfield, 1997; Milliman, 1974; Rosales et al., 2004). Universal values for this chemical screening probably cannot be adopted since the sedimentary, early diagenetic and late diagenetic chemical environments of each sediment type are different. In organic matter-rich, carbonate-poor sediments, very early diagenetic pyrite frequently occurs on the surface (or in voids) of the rostra. The process of pyrite formation should be of no serious effect on the carbonate chemical and isotopic data since no new carbonate is formed in this shallow diagenetic zone (cf. Rosales et al., 2004). Then, higher limits for Fe contents (when Mn and Sr contents are acceptable) can be adopted.

Detailed studies in the last several years have shown that both elemental compositions and stable isotope data (typically $\delta^{13}C$ values) of belemnite rostra are also partly influenced by biological fractionation and the life histories of individual species in different environments. Rexfort and Mutterlose (2006) studied C and O isotope ratios of cuttlebones from the cephalopod *Sepia officinalis* cultivated at a known temperature and those caught in the North Sea off Germany. Their data suggests that *Sepia* precipitates carbonate in oxygen isotopic equilibrium with seawater, reflecting the ambient temperature. Carbon isotope composition was influenced by biofractionation and showed no simple correlation to oxygen isotopes. Incorporation of isotopically light metabolic carbon also significantly affects the stable carbon isotope signal recorded in recent *Spirula spirula* (Price et al., 2009a). Belemnite records may behave similarly. McArthur et al. (2007a) studied paleoproxies (Mg/Ca, Sr/Ca, Na/Ca, $\delta^{13}C$, $\delta^{18}O$) in two species of well preserved coeval Toarcian belemnites. They found that Mg/Ca ratios are influenced by biofractionation, while Sr/Ca and Na/Ca ratios likely reflect climatic changes. The $\delta^{13}C$ and $\delta^{18}O$ values of the two species differed significantly (*Acrocoelites vulgaris* being 0.8‰ more positive in $\delta^{13}C$, and 1‰ more negative in $\delta^{18}O$ than *Acrocoelites subtenuis*, on average), which was interpreted as a result of these species living in different and restricted environmental niches. Price and Page (2008) studied molluscan and belemnite faunas from the Callovian/Oxfordian boundary in Dorset, UK. They found that belemnite $\delta^{18}O$ data and the resulting calculated paleotemperatures straddle the corresponding ranges for bivalves (*Gryphaea*) and ammonites. Therefore, belemnites probably migrated vertically through the water column, and different belemnite taxa likely inhabited different bathymetric niches. This assumption should be supported by comparative isotope analyses of species with different rostrum morphologies: long thin rostra reflecting a fast pelagic life, while stouter and short rostra possibly representing species living near the bottom or close to the shore. The dependence of Late Cretaceous belemnites on transgressive/regressive tracts (bathymetric valence) has also been recently demonstrated by Wiese et al. (2009). Wierzbowski and Joachimski (2009) studied two well preserved belemnite rostra (*Hibolithes beyrichi* and *H. hastatus*) from the Bathonian of Poland and observed differences in $\delta^{18}O$ data, interpreted as differences in habitat temperatures, while $\delta^{13}C$ fluctuations resulted from changes in metabolic activity. Fortunately, if a studied profile is dominated by one belemnite species, the importance of the biofractionation problem should be probably reduced: individuals of one species probably followed a similar style of life and imposed similar biofractionation on $\delta^{13}C$ data.

4. Studied sections, materials and methods

The positions of continents and the studied sites during the Late Jurassic/Early Cretaceous are shown in Fig. 1. Details on section

locations, lithology, biostratigraphy, and on the methods used to obtain paleomagnetic records used in this paper are contained in Houša et al. (1996, 1999, 2004), Chadima et al. (2006), Houša et al. (2007), Zakharov and Rogov (2008b), Pruner et al. (2010), and are given only briefly. Sedimentary rocks of all the studied sections are unmetamorphosed.

4.1. The Brodno section

The Brodno section (Michalík et al., 2009, and references therein; paleomagnetic study: Houša et al., 1996, 1999; geochemistry of sediments: Mizera and Řanda, 2009; present position: WGS84 coordinates 49°16′03″N, 18°45′12″E) was located at approximately 40°N during the Late Jurassic and Early Cretaceous (see maps of Scotese and Golonka, 1992; Smith et al., 1994; see Fig. 1). This section represents a record of hemipelagic marine carbonate sedimentation in a marginal zone (the Pieniny Klippen Belt) of the Outer Western Carpathians. It consists of fine-grained limestone composed mainly of calcitic micro- and nanoplankton tests, and covers an interval from the lower Tithonian to lower Berriasian. The paper of Michalík et al. (2009; Fig. 10 on page 225) contains bulk limestone C and O isotope data for 46 samples. The $\delta^{13}C$ values oscillate only very slightly from 1.29 to 1.53‰ V-PDB (average 1.45‰), while $\delta^{18}O$ values range from −2.60 to −0.88‰ V-PDB (average −1.62‰). The minor oscillations in $\delta^{13}C$ (in fact only slightly larger than the analytical error) were interpreted by Michalík et al. (2009) as reflecting the rhythmic character of the sequence and possibly also sea-level changes. The variation in carbonate $\delta^{18}O$ throughout the section was interpreted by these authors as resulting from temperature changes in the range of 15.5 to 21.3 °C (supposing a value of −1‰ V-SMOW for contemporaneous seawater), as well as possibly from periodic minor decreases in surface-water salinity (and thus also decreases in $\delta^{18}O$).

Since it was not clear if the data of Michalík et al. (2009) represent average samples taken throughout the whole thickness of each bed (with individual bed thicknesses of 5 to 25 cm), or if they are chip samples collected from a single point, we tested the within-bed C and O isotope variability by analyzing a detailed profile across bed C 18 (74 mm thick). The possible influence of early- and late-diagenetic features was further tested by analyzing detailed profiles perpendicular to a siliceous nodule, and perpendicular to a diagenetic calcite veinlet.

4.2. The Puerto Escaño section

The Puerto Escaño (GA-7) section was located at approximately 28°N during the Upper Jurassic and Lower Cretaceous (see maps of Smith et al., 1994, Fig 1; section biostratigraphy and magnetostratigraphy: Pruner et al., 2010; present day position: 37°26′30″N, 4°17′28″E). This section shows a succession of relatively uniform lithologies. From a paleogeographic point of view, it is a part of the External Subbetic Basin located close to the Variscan Iberia elevation. Sedimentary conditions correspond to a distal, epioceanic environment during the Late Jurassic and the earliest Cretaceous (Olóriz et al., 2004). The section is represented by bedded limestones (wackestones) with thin clayey limestone intercalations. The lower (predominantly Jurassic) part consists of Ammonitico Rosso and related facies, ranging from limestones to nodular clayey limestone horizons. Generally, the sedimentary environment of the Puerto Escaño section is markedly shallower than that of the Brodno section. These depositional conditions are recorded on raised blocks (swells) with evidence of omission surfaces (below the biostratigraphic resolution level, however). In addition, faunal assemblages of some horizons, containing brachiopods, echinoids, belemnites (genera *Hibolithes*, *Pseudobelus*), and fragments of molluscs (bivalves), suggest episodes of shallowing during sedimentation.

Sample positions within the section, shown in Table 1, are related to bed numbers, and the section readings in meters are identical to those in the study of Pruner et al. (2010). Altogether 46 samples of whole-rock and 5 samples of belemnite rostra were analyzed from this section.

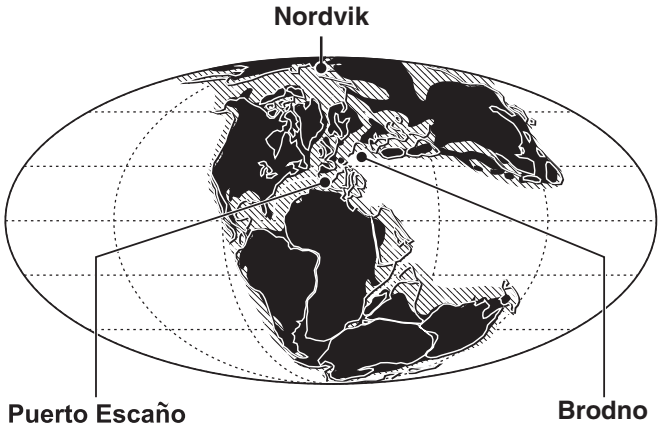

Fig. 1. Position of the studied sections in a paleogeograhic map, showing the positions of continents at the J/K boundary (from Scotese and Golonka, 1992).

4.3. The Nordvik section

The Nordvik section is located at approximately 74°N, which roughly corresponds to its position during the Late Jurassic/Early Cretaceous (see maps of Scotese and Golonka, 1992; and Smith et al., 1994; present position: 73°52′36″N, 113°08′33″E), making it one of northernmost accessible sections with continuous sedimentary succession around the J/K boundary. The locality was situated between the Middle Siberian elevation in the south and Tajmyr Island in the northwest during the sedimentation (Dzyuba et al., 2007; Zakharov and Rogov, 2008b). Lithology of the studied part of this section is quite different from that of the other two localities, consisting of marine silt- to clay-dominated deposits with diagenetic concretions and few diagenetically-cemented thin carbonate beds (Houša et al., 2007). These sediments have been interpreted as deposited in a lower sublittoral zone, at depths between 100 and 200 m. The whole section is rich in organic matter (2.19% organic C on average) and, with the exception of occasional concretions of diagenetic carbonates, poor in carbonate (0.82% carbonate C on average). Belemnite rostra are therefore the only material to be used for the production of primary C and O isotope data: genera *Cylindroteuthis* (72.2% of samples), *Lagonibelus* (14.8% of samples), *Pachyteuthis* (9.3% of samples), and *Simobelus* (3.7% of samples) enclosed within organic-rich mudstone. The reducing character of these sediments induced the widespread formation of diagenetic pyrite through a reduction of dissolved sulfate in pore water. Pyrite is also abundant at the surface of belemnite rostra, either covering the whole rostrum surface, or formed between the outer layers of concentric banding, and less commonly along the central line. Nevertheless, with the exception of these pyrite-enriched zones, the belemnite rostra are translucent, with well preserved radial arrangement of calcite crystals and clearly visible concentric banding. Similarly to Rosales et al. (2004), we consider the early diagenetic surface pyrite coatings on some of our belemnite samples as a factor which could help in their protection from post-depositional recrystallization. Altogether 54 samples of belemnite rostra were analyzed from the Nordvik section.

4.4. Analytical methods

During field sampling, the positions of all samples with respect to bed numbers were precisely recorded, as well as readings in meters

Table 1
Stable isotope data (bulk limestone) from the Puerto Escaño section.

Sample no.	Layer no.	Position in profile (m)	$\delta^{13}C$ (‰, V-PDB)	$\delta^{18}O$ (‰, V-PDB)
1	42	7.14	1.30	−1.29
2	41	6.95	1.14	−0.98
3	40 Upper part	6.76	1.32	−1.49
4	40/1	6.54	1.46	−1.64
5	40 B	6.37	1.47	−1.68
6	39	6.28	1.39	−1.47
7	38/1	6.09	1.44	−1.42
8	37	5.85	1.40	−1.44
9	36	5.57	1.36	−1.26
10	35 lower part	5.48	1.41	−1.45
11	35 lower part	5.23	1.39	−1.56
12	34B	5.02	1.43	−0.96
13	34A	4.91	1.37	−1.41
14	33C	4.85	1.32	−1.31
15	33B	4.73	1.37	−1.60
16	33A	4.63	1.31	−1.23
17	32B upper part	4.54	1.33	−0.91
18	32A	4.42	1.23	−0.88
19	31/2	4.31	1.35	−1.00
20	30 sv.	4.21	1.36	−0.97
21	29	4.10	1.42	−1.13
22	28/1	4.00	1.48	−1.85
23	27	3.80	1.40	−1.13
24	26B	3.61	1.42	−1.44
25	26A	3.46	1.31	−1.30
26	25	3.29	1.37	−1.39
27	24	3.11	1.50	−1.32
28	23B	2.90	1.31	−0.87
29	22B	2.69	1.34	−0.84
30	21	2.12	1.44	−1.13
31	20	2.07	1.49	−1.25
32	19	2.02	1.46	−1.44
33	18/2	1.96	1.44	−1.55
34	17	1.87	1.45	−1.54
35	16	1.78	1.44	−1.21
36	15	1.70	1.42	−0.86
37	14C upper part	1.59	1.37	−0.95
38	14B	1.53	1.44	−1.15
39	14A	1.46	1.43	−1.04
40	13B	1.36	1.38	−1.40
41	13A	1.22	1.41	−0.40
42	12	1.14	1.47	−1.39
43	11	0.99	1.52	−1.46
44	10	0.83	1.44	−1.27
45	9	0.71	1.53	−1.22
46	8	0.63	1.24	−0.57

from an arbitrary measuring point in each section. We used the same bed numbering and section scale in meters as Michalík et al. (2009) for Brodno, Pruner et al. (2010) for Puerto Escaño, and Zakharov and Rogov (2008b) for Nordvik.

Bulk limestone samples from the Puerto Escaño section were sampled as ~5 g chip samples from homogeneous central parts of each bed, taken from freshly broken rock surfaces. Detailed profiles at Brodno were sampled from fresh rock surfaces using a micro-drill.

Belemnite samples from the Nordvik and Puerto Escaño sections were examined under a binocular microscope, and suitable specimens were separated either by micro-drilling or by handpicking of suitable chips. Parts of rostra from the outermost concentric growth bands and along the apical line were avoided during the sampling, as well as any rostra sections showing growth of early diagenetic pyrite.

Carbonate samples were then homogenized in an agate mortar. C and O isotope compositions were determined using a standard 100% H_3PO_4 digestion under vacuum at 25 °C, followed by measurement on a Finnigan MAT 251 mass spectrometer in the laboratories of the Czech Geological Survey in Prague. Replicate analyses (including sub-samples that were newly separated from the field samples) were performed for randomly selected rock and belemnite samples. In all cases, the difference between original and replicate analyses was smaller than the analytical error (±0.1‰). All stable isotope data used in this paper, i.e. new data for the Nordvik and Puerto Escaño sections, supplementary data from the Brodno section, and published data of the Brodno section taken from Michalík et al. (2009), were measured at the same laboratory (the Stable Isotope Laboratory of the Czech Geological Survey, Prague) using the same internal and external standards, with identical analytical error below ±0.1‰ for both $\delta^{13}C$ and $\delta^{18}O$ values.

Due to the possible Mn and Fe incorporation into the belemnite carbonate from diagenetic pore waters, all samples derived from belemnites were additionally analyzed for Ba, Ca, Fe, Mg, Mn, Na and Sr. Separated aliquots (weighing 20 to 40 mg) from the homogenized belemnite samples were dissolved in 10 ml 20% HCl (Ultrapure, Merck) and brought up to 100 ml with re-distilled water. After filtration through a 0.45 um Nylon filter, concentrations of metal cations were determined by inductively coupled plasma optical emission spectrometry (ICP EOS, Iris Intrepid 2 Duo). The plasma and instrument parameters were set according to the manufacturer's recommendations. The instrument was calibrated with a mixed standard solution prepared from 1000 ppm certified single element standards (Analytika, Prague).

The dating of samples is based on magnetostratigraphic studies of Houša et al. (1996, 1999) at Brodno, Pruner et al. (2007) and Pruner et al. (2010) at Puerto Escaño, and Chadima et al. (2006) and Houša et al. (2007) at Nordvik. Geomagnetic polarity zones found by these authors were assigned to polarity intervals given by the Geomagnetic Polarity Time Scale 2004 (Gradstein et al., 2004). Based on the identified polarity zones, a numerical age was assigned to an arbitrary level of each section using a smoothing spline interpolation. For the Nordvik section, the depositional rate could not be fitted by a single spline function, so the section was instead split into three intervals, namely 38.36 to 45.06 m, 45.06 to 46.56 m, and 46.56 to 51.46 m, with an almost constant depositional rate for each interval.

5. Results

Results of new stable isotope analyses of bulk limestone from the Puerto Escaño section are shown in Table 1 and Fig. 2, the relationship between $\delta^{13}C$ and $\delta^{18}O$ data of limestones and belemenites for the Puerto Escaño section in Table 2, isotope analyses and rostrum chemistries of samples from the Nordvik section in Table 3 and Fig. 3, and additional stable isotope analyses of bulk limestone rocks from the Brodno section in Table 4.

Bulk limestone data from the Puerto Escaño section show only a very limited variation ($\delta^{13}C$ values from 1.14 to 1.53‰ V-PDB, average 1.39; $\delta^{18}O$ values from −1.85 to −0.40, average −1.24‰ V-PDB). The range and the average of carbon isotope data are very similar to the bulk carbonate data of the Brodno section reported by Michalík et al. (2009), where $\delta^{13}C$ values slightly oscillate in the range from 1.29 to 1.53‰ V-PDB (average 1.45‰). The $\delta^{18}O$ values of the two sections differ slightly (Fig. 4), with a slightly narrower range for the Brodno section ($\delta^{18}O$ −2.60 to −0.88‰ V-PDB; average −1.62‰). Several well preserved belemnite rostra analyzed from the Puerto Escaño section (Table 2) show a systematic difference from the host limestone, with lower $\delta^{13}C$ but higher $\delta^{18}O$ values compared to their host rock (Fig. 5).

Additional stable isotope analyses from the Brodno bulk limestone (Table 4) showed only very limited within-bed variability, and only small variations in short profiles sampled perpendicular to the diagenetic veinlet and siliceous nodule. Obtained data are in good agreement with the measurement of Michalík et al. (2009) from the same bed, thus supporting the overall data reliability.

Typically low Mn concentrations (<150 ppm) but frequently higher Fe concentrations (average 290 ppm) were found for belemnite samples from the Nordvik section. This is most probably a result

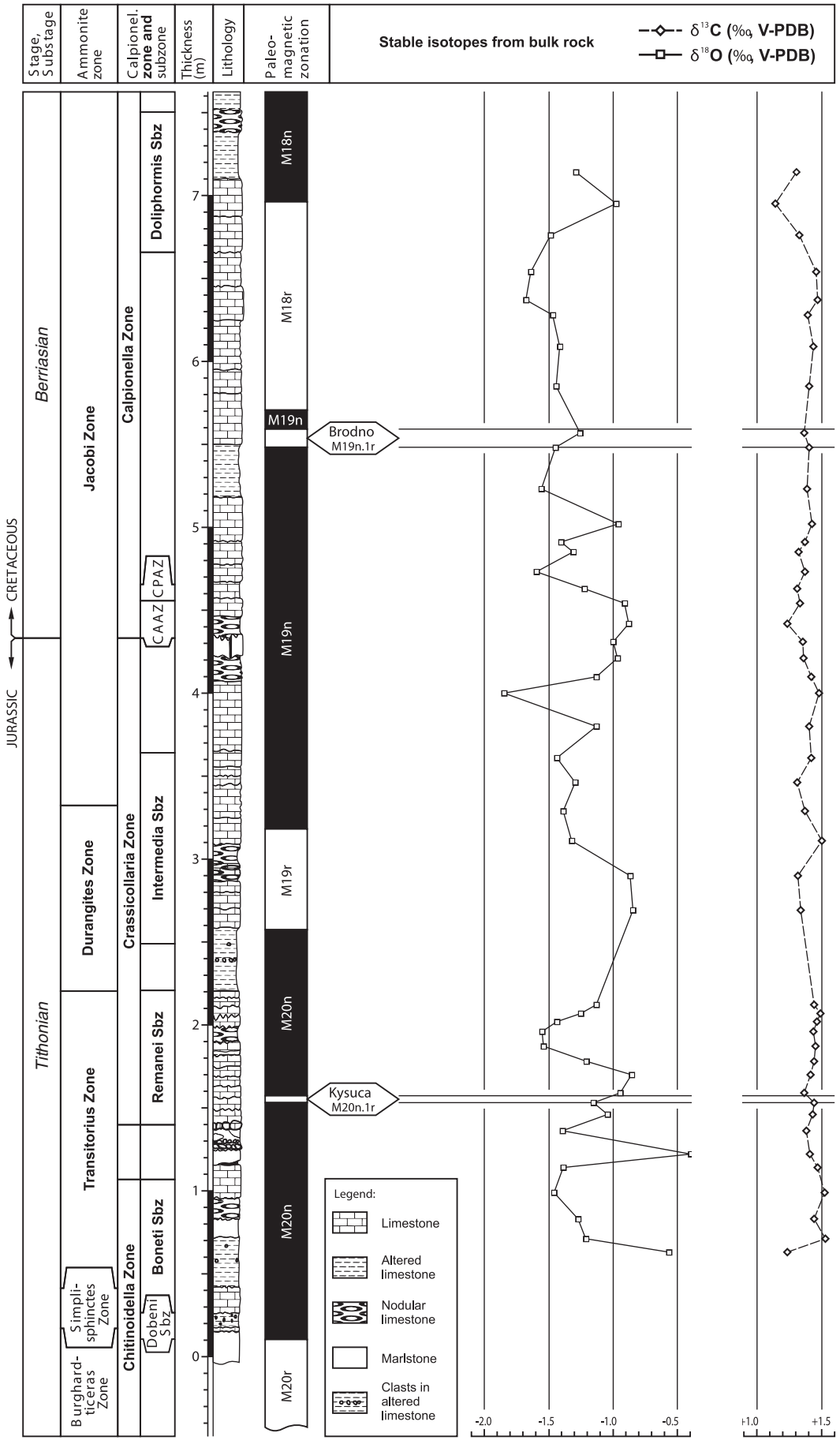

Fig. 2. Stable isotope signals at the Puerto Escaño section. Lithology, biostratigraphy, magnetostratigraphy, and the position of the J/K boundary follow Pruner et al. (2010).CAAZ - Calpionella alpina acme zone, CPAZ - Crassicollaria parvula acme zone.

Table 2
Comparison of stable isotope data for limestone and belemnite rostra, Puerto Escaño section.

Layer no.	$\delta^{13}C$ limestone (‰, V-PDB)	$\delta^{18}O$ limestone (‰, V-PDB)	$\delta^{13}C$ belemnite (‰, V-PDB)	$\delta^{18}O$ belemnite (‰, V-PDB)
33B	1.36	−1.55	−1.14	−0.09
21	1.44	−1.13	−0.29	0.51
22B	1.34	−0.84	−1.48	−0.01
23B	1.31	−0.87	−1.11	0.35
42	1.31	−1.29	−0.82	−0.10

of the fact that some parts of the belemnite rostra are partly replaced by abundant early diagenetic pyrite. Pyrite was mostly formed under conditions of bacterial sulfate reduction very early in diagenesis, when rostrum carbonate was partly corroded and no new carbonate deposition occurred. This process cannot be therefore expected to affect C and O isotope chemistry of the rostrum carbonate. Mn contents, reflecting deeper diagenetic influence, were used for sample screening: samples with >150 ppm Mn were excluded from further interpretation. The chosen limit value is in agreement with that found in a detailed study by Rosales et al. (2004) for nondisturbed sections of the studied Early Jurassic belemnite rostra. All analyzed samples (including those excluded from further processing based on their Mn contents) had Sr contents above 900 ppm, with an average value of 1780 ppm Sr. The Mn and Sr contents of all samples selected for further interpretation were therefore lying in the range typical for modern low-magnesium shells (Sr in modern shells 800 to 2800 ppm, Mn 0 to 500 ppm; Veizer et al., 1999). No correlation between the

Table 3
Stable isotope data (belemnite rostra, in ‰ vs. V-PDB) and sample chemical compositions (in ppm) from the Nordvik section. Data in italics (Mn content>150 ppm) are considered to come from diagenetically affected samples; they were not used for either figures or subsequent analyses.

Field sample no.	Position in profile (m)	Belemnite species	$\delta^{13}C$ (‰)	$\delta^{18}O$ (‰)	Ba (ppm)	Ca (ppm)	Fe (ppm)	Mg (ppm)	Mn (ppm)	Na (ppm)	Sr (ppm)
H 420	52.06	*Cylindroteuthis knoxvillensis*	0.48	−0.27	226	374,576	185	12,176	73	6129	2046
H 380	51.66	*Cylindroteuthis* sp. ?	0.36	−0.75	260	428,629	139	13,468	53	6524	1843
H 240	50.26	*Cylindroteuthis* sp.	0.29	−0.95	419	400,389	97	13,016	65	6249	1486
H 230	50.16	*Cylindroteuthis* sp. ?	0.29	−1.08	160	370,978	194	8757	117	4196	1276
H 202	49.88	*Cylindroteuthis* sp. ?	0.67	−0.15	238	384,053	170	12,821	88	5668	1514
H 180	49.66	*Cylindroteuthis* sp.	0.39	−1.57	316	400,794	216	17,079	65	9032	1956
H 155	49.41	*Cylindroteuthis* sp.	−1.15	−0.74	215	344,818	277	10,339	104	6467	2096
H 145	49.31	*Cylindroteuthis* sp.	0.03	−0.03	190	376,385	164	10,356	70	4983	1545
H 140	49.26	*Cylindroteuthis* sp.	0.72	−0.55	199	382,534	158	10,469	45	4966	1688
H 137	49.23	*Cylindroteuthis* sp. ?	0.64	0.47	153	371,698	115	7618	45	4505	1808
H 130	49.16	*Cylindroteuthis* cf. *knoxvillensis*	0.06	−0.18	191	379,389	173	8443	91	5204	1969
H 80	48.66	*Cylindroteuthis* sp. ?	*0.01*	*−0.92*	*121*	*380,310*	*440*	*6978*	*208*	*3518*	*1516*
H 50	48.36	*Cylindroteuthis* sp.	0.55	−0.16	400	387,125	463	12,946	84	7233	2103
H 40	48.26	*Cylindroteuthis* sp. ?	0.62	−0.94	103	364,991	113	5619	44	3179	1507
H 10	47.96	*Cylindroteuthis* sp.	1.04	−1.15	220	384,643	135	10,239	61	4364	1733
D 28	47.58	*Cylindroteuthis* sp.	0.34	0.08	135	375,879	167	7111	79	5013	1628
D 45	47.41	*Cylindroteuthis* sp. ?	0.12	−0.17	138	379,292	124	7515	29	3545	1302
D 173	46.13	*Cylindroteuthis porrectiformis*	−0.03	−0.68	109	376,964	188	5166	60	2780	1686
D 640	41.46	*Cylindroteuthis porrectiformis*	*0.22*	*0.01*	*109*	*275,199*	*44,862*	*8431*	*758*	*3413*	*1078*
D 655	41.31	*Cylindroteuthis* sp. ?	*0.63*	*−1.06*	*222*	*377,581*	*4785*	*8823*	*347*	*5127*	*1649*
D 760	40.26	*Pachyteuthis* sp. ?	1.64	0.07	328	398,382	926	12,340	68	5535	1799
D 930	38.56	*Cylindroteuthis* sp. ?	0.88	−0.95	445	402,768	198	14,987	37	6875	1672
D 950	38.36	*Pachyteuthis* sp. ?	0.33	−1.15	317	405,159	120	12,171	47	5718	1721
D 1030	37.56	*Lagonibelus sibiricus*	0.38	0.83	273	390,217	234	10,293	51	5134	1974
D 1040	37.46	*Cylindroteuthis sp.*	0.51	−0.28	272	395,058	236	9125	56	4677	1583
D 1300–1320	34.76	*Cylindroteuthis* cf. *comes*	−0.02	1.11	336	407,788	159	13,429	44	8147	2510
D 1430–1475	33.34	*Cylindroteuthis* cf. *jacutica*	0.98	−0.68	317	399,449	396	12,136	55	5932	2275
D 1480	33.06	*Cylindroteuthis* sp.	−0.60	0.70	223	387,419	158	7952	55	4848	2377
D 1530	32.56	*Cylindroteuthis* cf. *comes*	−0.56	0.08	383	406,745	605	13,302	103	6986	2639
D 1540	32.46	*Cylindroteuthis* cf. *jacutica*	−0.47	0.25	424	409,025	733	14,674	136	7208	1712
D 1570	32.16	*Cylindroteuthis lenaensis*	−0.07	1.29	329	392,279	712	11,482	96	6993	1948
D 1610	31.76	*Cylindroteuthis* sp.	0.60	−0.24	332	401,739	242	12,326	87	5065	1949
D 1650	31.36	*Lagonibelus parvulus*	−0.09	0.64	352	405,285	106	12,732	46	5862	1853
D 1870	29.16	*Simobelus* sp.	−0.58	−0.77	358	403,964	932	13,446	103	6739	1754
D 1930	28.56	*Simobelus* sp.	0.62	0.27	366	400,857	542	12,073	104	5996	1770
D 1930	28.56	*Cylindroteuthis aff. porrectiformis*	0.77	0.55	308	401,198	286	11,050	60	5335	1976
D 2030	27.56	*Cylindroteuthis* sp.	1.07	0.15	329	393,878	834	9466	129	4933	1716
D 2030	27.56	*Cylindroteuthis* sp.	0.74	−0.27	304	392,883	258	10,925	65	5075	1754
D 2430	23.56	*Cylindroteuthis* cf. *sachsi*	−0.28	0.77	520	405,352	370	15,108	144	7634	2382
D 2530	22.56	*Cylindroteuthis* sp.	2.42	1.10	190	402,863	99	11,357	44	5427	2104
D 2630	21.56	*Cylindroteuthis obeliscoides*	2.49	−0.44	377	404,558	82	14,265	43	6986	1913
D 2730	20.56	*Lagonibelus* cf. *strigatus*	1.31	−0.61	303	394,212	263	11,662	76	5270	1466
D 2980–3000	17.96	*Cylindroteuthis urdjukhaensis*	*0.81*	*1.05*	*415*	*394,977*	*320*	*13,609*	*327*	*6135*	*1880*
D 3080–3085	17.04	*Cylindroteuthis* sp.	0.83	1.38	407	396,715	315	13,062	112	6004	1394
D 3130	16.56	*Cylindroteuthis* sp.	0.92	0.67	371	404,297	188	12,754	68	6105	2012
D 3230	15.56	*Cylindroteuthis* sp.	1.45	1.15	475	404,910	372	13,824	71	6086	1820
D 3330	14.56	*Lagonibelus strigatus*	1.60	−0.71	334	398,025	236	11,671	90	5235	1785
D 3530	12.56	*Lagonibelus* cf. *nordvikensis*	0.57	0.41	385	405,534	467	13,162	107	6269	1773
D 3630–3635	11.54	*Lagonibelus* cf. *nordvikensis*	1.31	1.28	306	401,026	160	11,731	45	5432	1631
D 3930	8.56	*Lagonibelus* cf. *nordvikensis*	2.25	0.52	381	401,902	332	13,873	99	6356	2222
D 4030–4035	7.54	*Cylindroteuthis* sp. ?	2.31	1.61	402	410,769	169	13,683	41	6813	1694
D 4200	5.86	*Pachyteuthis* cf. *excentralis*	2.73	0.96	197	391,826	374	7989	77	5114	1343
D 4380	4.06	*Pachyteuthis* cf. *panderiana*	3.10	0.51	266	393,077	10	10,242	42	6096	902
D 4480	3.06	*Pachyteuthis* cf. *panderiana*	1.03	1.58	282	395,502	163	10,128	50	5024	1321

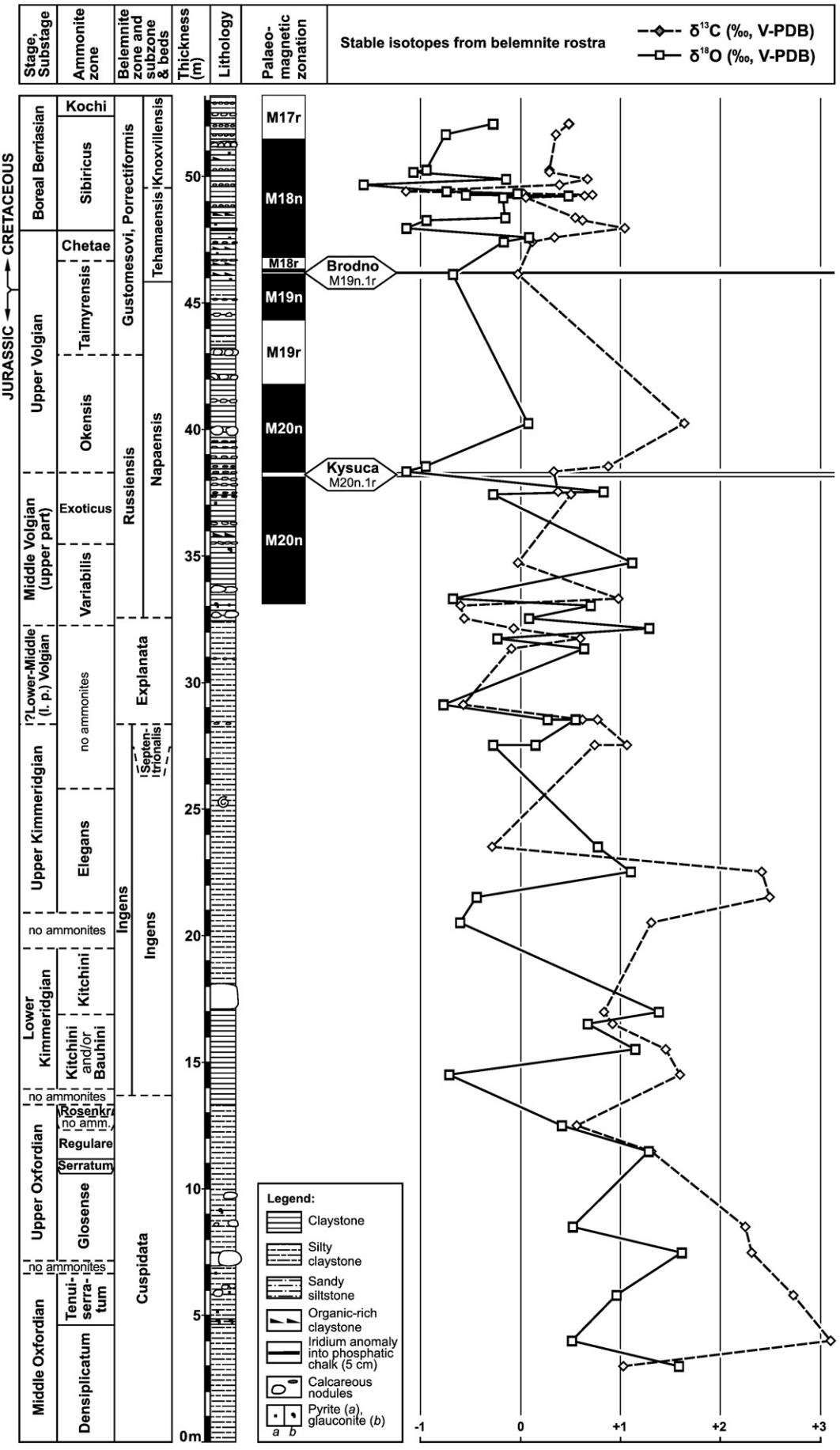

Fig. 3. Stable isotope signals at the Nordvik section. Lithology, biostratigraphy, magnetostratigraphy, and the position of the J/K boundary follow Houša et al. (2007).

Table 4
Additional stable isotope data from the Brodno section, detailed profiling perpendicular to a bed boundary, to a diagenetic veinlet and to a siliceous nodule.

Sample no.	Description	$\delta^{13}C$ (‰, V-PDB)	$\delta^{18}O$ (‰, V-PDB)
i. Detailed profile accross the layer no. C18			
44/1	1 mm from base	1.40	−1.70
44/2	12 mm from base	1.36	−1.82
44/3	25 mm from base	1.37	−1.86
44/4	35 mm from base	1.38	−2.05
44/5	45 mm from base	1.33	−2.07
44/6	60 mm from base	1.38	−1.83
44/7	74 mm from base	1.26	−1.77
ii. Detailed profile perpendicullar to white diagenetic calcite veinlet, layer no. C23			
52/1	A white veinlet	1.56	−2.91
52/2	1–2 mm from the contact of the veinlet	1.43	−2.22
52/3	10 mm from the contact of the veinlet	1.45	−1.99
iii. Detailed profile perpendicullar to a surface of siliceous nodule, layer no. C35			
62/1	At the contact with siliceous nodule	1.36	−2.97
62/2	3 mm of the contact	1.33	−2.94
62/3	15 mm of the contact	1.34	−2.71

ratio and the stable isotope data was observed for the belemnites from Nordvik, and the variation in Mg content in the rostra is low.

Several excursions and trends were observed at the Nordvik section, where a much longer stable isotope profile was analyzed. The sampled interval covers a period from the middle Oxfordian to the basal Boreal Berriasian. Two positive excursions were found in the lower part of the section (in the middle Oxfordian and in the basal part of the upper Kimmeridgian) reaching up to $\delta^{13}C$ of +3‰ (V-PDB), unfortunately represented only by a small number of analyzed samples (Fig. 3). Because these peaks occur at similar positions as positive excursions in the belemnite record of the Russian Platform described by Price and Rogov (2009), we interpret them to reflect changes in carbon isotope composition of marine bicarbonate, and not biofractionation. Similar middle Oxfordian positive carbon isotope excursions have been documented also in the Western Carpathians by Wierzbowski (2004). Two negative $\delta^{13}C$ excursions in the Kimmeridgian of the Nordvik section are fixed approximately at the same level, as observed in Subpolar Urals (Zakharov et al., 2005): minor in the middle part of the lower Kimmeridgian and more significant in the upper Kimmeridgian *Elegans* ammonite zone. Moreover, there is an irregular $\delta^{13}C$ decrease throughout the whole of Upper Jurassic, which is a trend that has been seen at many other sections.

The belemnite $\delta^{18}O$ data show an irregular decrease from values as high as +1.6‰ in the middle Oxfordian to values between 0 and −1‰ in the upper Volgian, similarly to that documented for the Upper Jurassic of the Russian Platform by Price and Rogov (2009). There is also a partial overlap in the belemnite genera present in the Russian Platform (Price and Rogov, 2009) and those of the Nordvik section. A narrower data scatter in both $\delta^{13}C$ and $\delta^{18}O$ within ±1‰ is abundant at Nordvik, but these oscillations are difficult to correlate with those at other sections due to their relatively high frequency.

6. Data interpretation and discussion

6.1. Oxygen isotopes and temperature estimates

It is generally accepted that the interpretation of oxygen isotope data from marine carbonates (if the influence of diagenetic and epigenetic processes is reduced by careful sample screening) requires solving a paleotemperature equation with two unknowns (carbonate $\delta^{18}O$ and seawater $\delta^{18}O$ values), of which only one can be directly measured. A 1‰ difference in the selected $\delta^{18}O$ seawater value results in a ~4 °C difference in the calculated temperature. One frequently used approach is to use a seawater value of −1‰ (V-SMOW), which should be the average ocean water value of the post-Jurassic polar ice-free world (Gröcke et al., 2003; Lécuyer and Allemand, 1999; Shackleton and Kennett, 1975). Of the published paleotemperature equations, that of Anderson and Arthur (1983) is frequently used:

$$T(^{\circ}C) = 16.0 - 4.14(\delta c - \delta w) + 0.13(\delta c - \delta w)^2$$

This approach should be considered only a rough approximation since the variation in seawater $\delta^{18}O$ of shallow epicontinental seas or seas poorly communicating with the ocean can vary by as much as ±2‰ or more (cf., e.g. Rohling, 2007). The study of Broecker (1989) indicated differences as large as 1.5‰ between low and high latitudes in the open ocean under glacial conditions. Moreover, the interpretation is complicated by the fact that the individual animal groups usually occupy quite different depth niches, with different temperatures.

The use of bulk-rock $\delta^{18}O$ carbonate data for temperature calculation is further complicated by a possible alteration of the original record by diagenetic changes and carbonate recrystallization during lithification. The carbonate $\delta^{18}O$ data are generally shifted to lower values during meteoric water invasion and/or during increasing

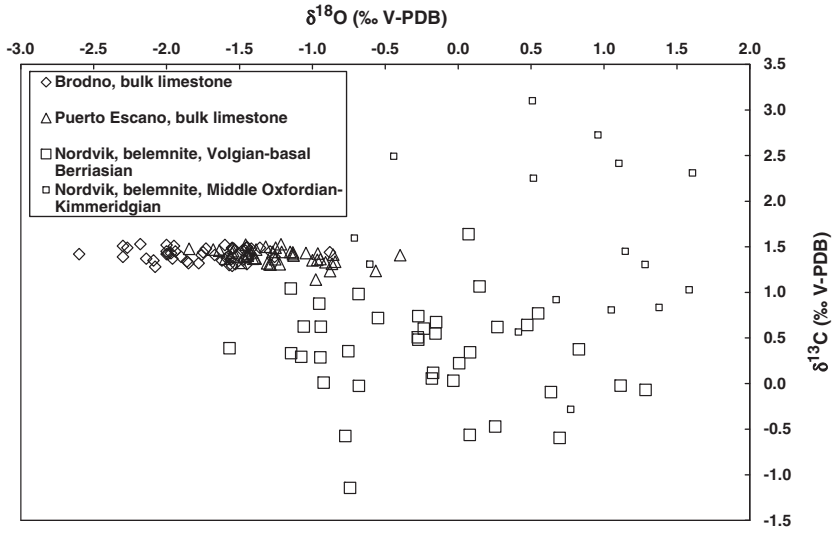

Fig. 4. C and O isotope data of the Brodno, Puerto Escaño, and Nordvik sections in the $\delta^{13}C$ vs. $\delta^{18}O$ diagram. Data from the upper part of the studied section at Nordvik (above the Kimmeridgian/Volgian boundary) are shown by larger symbols.

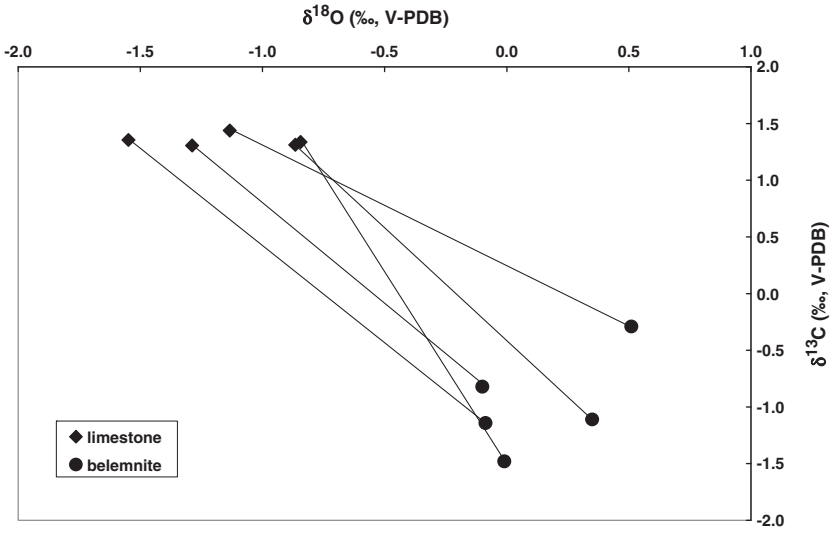

Fig. 5. Comparison of bulk limestone and belemnite C and O isotope data from the Puerto Escaño section. Individual pairs host rock–belemnite are connected by a line.

diagenetic temperature (and the calculated temperatures shift to higher values). The temperatures calculated from bulk-rock can be therefore considered only an upper limit of the possible depositional temperatures.

Using this simplified model approach (i.e., supposing a well preserved stable isotope record, temperature-controlled oxygen isotope equilibrium between carbonate and seawater, and a value of −1‰ V-SMOW for seawater), the temperatures shown in Table 5 can be calculated. This calculation is unfortunately of rather limited importance because seawater $\delta^{18}O$ was not identical at all studied localities and probably not constant over time (see also Price and Rogov, 2009). On the other hand, the constant presence of diverse cephalopod associations throughout the Late Jurassic in the Nordvik area indicates normal marine salinity. Moreover, it is highly probable that some belemnite species frequently migrated (or permanently lived) in deeper, cooler water (Saks and Nalnyaeva, 1979; Zakharov et al., 2006). Contrasting behavior of individual belemnite genera are expected to be reflected by specific rostrum morphologies (see Section 3), and some rostra can even indicate day and night cycles (possibly as a result of vertical migrations; Dunca et al., 2006). The temperature estimates are thus of only limited precision.

6.2. Oxygen isotope data from Tethyan bulk-rock samples

A remarkable feature is the systematic difference between bulk limestone $\delta^{18}O$ data from the Brodno and Puerto Escaño sections, both located in the Tethyan Realm. As indicated by data homogeneity throughout each of the sections, the performed check of the within-bed variability, and the variability in detailed profiles perpendicular to siliceous concretion and a diagenetic veinlet (see Table 4), the observed difference between the sections is probably of primary marine origin rather than a result of diagenetic overprint. As indicated by some other studies (Bodin et al., 2009), whole-rock $\delta^{18}O$ data from an individual section can be all shifted in a similar style, with the trends and positions of individual excursions being preserved. Fortunately, the fine-grained limestones of the Brodno and Puerto Escaño sections are of very low porosities (after compaction and lithification), and the deep diagenetic and/or epigenetic overprint was therefore of only minor importance. Excluding the effect of diagenetic overprint, two other explanations are possible: a slightly higher temperature at Brodno than at Puerto Escaño, or higher $\delta^{18}O$ (i.e., salinity) of seawater at Puerto Escaño. Based on lithology and the fossil assemblage (with more benthic organisms), the depositional environment at Puerto Escaño was a shallower-water one compared to the Brodno section. Another possibility is the influence of lower-temperature currents at Puerto Escaño.

Based on the analyses of oxygen isotopes in phosphates of aquatic or semiaquatic vertebrate remains (fish, turtles, and crocodilians) from the famous Late Jurassic lithographic limestones, Billon-Bruyat et al. (2005) concluded that coastal marine waters were thermally homogeneous at the regional scale of Western Europe. Lécuyer et al. (2003) found different $\delta^{18}O$ levels for western and eastern parts of the Tethys in the Middle Jurassic (middle and late Bathonian), and interpreted this as a result of the influence of cold currents from the Arctic during an opening of the North Sea rift. Unfortunately, definite interpretation of these bulk-rock $\delta^{18}O$ data is impossible since diagenetic influence has always to be taken into account.

Table 5
Model calculation of paleotemperatures. The temperatures calculated from the bulk-rock samples (in parentheses) could have been influenced by diagenetic changes and represent the upper limit of possible temperatures. See the text for further explanation.

Brodno section (bulk limestone, model calculation supposing no diagenetic changes, calculation of Michalík et al., 2009)	(15.5 to 23.0 °C)	(Average 19.2 °C) (46 samples)
Puerto Escaño section (bulk limestone, model calculation supposing no diagenetic changes)	(14.2 to 19.6 °C)	(Average 17.1 °C) (46 samples)
Puerto Escaño section (belemnite)	10.0 to 12.4 °C	Average 11.5 °C (5 samples)
Nordvik (lower part of the section Middle Oxfordian to Lower Kimmeridgian)	6.1 to 14.8 °C	Average 9.4 °C (16 samples)
Nordvik (Upper Kimmeridgian to Boreal Berriasian)	7.8 to 18.4 °C	Average 13.0 °C (38 samples)

6.3. Oxygen isotope data at the Nordvik section

The clear trend toward lower carbonate $\delta^{18}O$ during the Late Jurassic at Nordvik corresponds to that observed earlier for the Russian Platform (Price and Rogov, 2009) and Scotland (Nunn et al., 2009). It is usually explained by a significant temperature increase from the Callovian and early and middle Oxfordian to the Kimmeridgian and Tithonian. Data equally support the possibility of decreasing latitudinal climatic gradients (climatic zoning) during the Late Jurassic. This is in agreement with records of ocean

Fig. 6. Stable isotope signals at the Brodno, Puerto Escaño, and Nordvik sections after recalculation of sample positions relative to chronological ranges of the individual magnetozones given by Gradstein et al. (2004). See the text for further details on this procedure. All isotope data are given in ‰ of the V-PDB standard.

temperatures in the Northern Hemisphere based on isotope data obtained from fish and shark tooth enamel (Dromart et al., 2003; Lécuyer et al., 2003), which indicate severe cooling and subsequent warming during the Middle–Late Jurassic transition in Europe. It is probable that our Nordvik data do not include the coldest period of this Middle–Late Jurassic transition, or, alternatively, such cooling was of only regional significance, reflecting changes in paleoceanography and paleocurrent pattern in Europe.

The subsequent continued carbonate $\delta^{18}O$ decrease toward the J/K boundary is in agreement with the common interpretation of the Late Jurassic and especially Kimmeridgian in which global temperature reached one of its maxima (Abbink et al., 2001; Frakes, 1979; Valdes and Sellwood, 1992; Zakharov et al., 2005), probably as a result of the greenhouse effect. Price et al. (2009b) calculated surface-water temperatures in excess of 30 °C based on $\delta^{18}O$ analyses of well preserved Late Jurassic fish otoliths from the United Kingdom, albeit such high paleotemperatures perhaps reflect decreasing salinity in ambient water due to regular migration of fish to brackish or fresh water, which is supported by carbon isotope data.

6.4. Carbon isotopes

Carbon isotope data from bulk limestone samples of the Puerto Escaño section show only a limited variation (Fig. 2), similar to the smooth isotope trends demonstrated earlier from other J/K boundary sequences (Gröcke et al., 2003; Michalík et al., 2009; Tremolada et al., 2006; Weissert and Channell, 1989; Weissert and Lini, 1991; Weissert and Mohr, 1996). Juxtaposition of isotope data from the Puerto Escaño and Brodno sections based on paleomagnetic record is shown in Fig. 6. Oscillations of the $\delta^{13}C$ curve within the short time interval studied only slightly exceed the analytical error of ±0.1‰. Unfortunately, the sampling density in this short, paleomagnetically correlated interval at Nordvik is low due to the rarity of belemnites in this part of the section.

Our analysis of a much longer part of the Nordvik section enabled to correlate several positive $\delta^{13}C$ excursions with those already known from the Tethyan Realm and Russian Platform. The positions of positive carbon isotope excursions in the middle Oxfordian and in the basal part of the upper Kimmeridgian can be correlated with similar events documented for the Tethyan Realm (e.g., Weissert and Mohr, 1996), as well as the Russian Platform (Price and Rogov, 2009). The high early Oxfordian $\delta^{13}C$ values may reflect the widespread deposition of organic-rich marine sediments which predate the Middle–Late Jurassic transition at ca. 160 Ma (Dromart et al., 2003). Unfortunately, the nature of carbon cycling in the atmosphere and oceans is extremely complex (Hansen and Wallmann, 2003; Wallmann, 2001; Weissert and Erba, 2004), with seawater $\delta^{13}C$ values being mainly controlled by the turnover of particulate organic carbon, as well as by influxes of isotopically light carbon from the continents in areas close to coasts. The $\delta^{13}C$ curve at Nordvik shows other minor positive excursions just above the M20n.1r (Kysuca) and M19n.1r (Brodno) magnetosubzones, which probably correspond to elevated particulate carbon deposition or to subdued carbon flux from continents. As documented in Section 3 of this paper, biofractionation can be responsible for at least some of the observed oscillations in $\delta^{13}C$ of belemnites as well. Nevertheless, the variation in $\delta^{13}C$ of one genus, e.g. *Cylindroteuthis* sp., from Nordvik is +2.49 to −1.15‰ (V-PDB), which is significantly wider than the biofractionation-induced variation reported for a single genus. An important part of the observed variation is therefore interpreted as being related to changes in carbon isotopic composition of the marine bicarbonate.

6.5. A comparison of C and O isotope data for bulk limestone and belemnite rostra

Table 2 and Fig. 5 show the relationships between the C and O isotope compositions of fine-grained host pelagic limestone and the belemnite rostra it contains (*Hibolithes*, *Pseudobelus*) from the Puerto Escaño section. In total, 5 such pairs were analyzed, with similar results. In all cases, the $\delta^{13}C$ values of limestone were higher (differences of +1.73 to +2.82‰) than those of the belemnite, and the $\delta^{18}O$ values of limestone were lower (differences of −0.83 to −1.64‰) than those of the belemnite. Similar differences between the whole-rock and belemnite isotope data have been also observed by Bodin et al. (2009). Biofractionation of carbon isotopes in belemnites has been already well documented (McArthur et al., 2007a; Wierzbowski and Joachimski, 2009). We interpret this difference in oxygen isotopes as a result of belemnites living in (or frequently visiting) deeper waters, similar to the interpretation of Price and Page (2008). The differences between the belemnite and limestone $\delta^{18}O$ values, ranging from 0.83 to 1.64‰, could reflect ambient temperature differences of 5 to 7 °C (supposing identical seawater $\delta^{18}O$, isotopic equilibrium, and well preserved records). It is generally accepted that belemnites were able to live at, or to visit, depths of up to 200 m, which is deep enough to produce such differences in $\delta^{18}O$ values. Diagenetic changes of the bulk-rock $\delta^{18}O$ represent another possible explanation.

7. Conclusions

1. Paleomagnetic correlation of stable isotope records was tested as a promising method for sections located in the Tethyan Realm (the Brodno section, Slovakia, and the Puerto Escaño section, Spain; bulk limestones), and in the Boreal Realm (the Nordvik section, Northern Siberia, Russia; belemnites). This correlation was complicated by the different lithologies of the sections and by the rarity of belemnites in the important part of the Nordvik section.
2. The Brodno and Puerto Escaño carbon isotope records are practically identical as for their absolute $\delta^{13}C$ values and their variation. Paleomagnetically correlated curves show similar patterns. The $\delta^{18}O$ values of the Brodno and Puerto Escaño sections also show similar magnitudes of oscillation, although they slightly differ. This difference may result from the differences in temperature and/or seawater $\delta^{18}O$ in the two regions, or from differences in diagenetic overprint.
3. Bulk limestone–belemnite pairs from the Puerto Escaño section show a systematic difference in both the $\delta^{13}C$ and $\delta^{18}O$ values for belemnites and limestone. This is interpreted as a result of a deeper-water life of belemnites (down to 200 m) and consequent lower temperatures derived for the oxygen isotopes, and as a result of belemnite biofractionation in the case of carbon isotopes.
4. The analyzed section at Nordvik covered a longer time interval (middle Oxfordian–earliest Boreal Berriasian) and allowed the correlation of pronounced positive carbon isotope excursions in the middle Oxfordian and in the early late Kimmeridgian with similar oscillations from the Russian Platform and Tethyan Realm.
5. The entire studied part of the Upper Jurassic stable isotope record at Nordvik shows irregular (oscillating) decrease in both $\delta^{13}C$ and $\delta^{18}O$ values towards the J/K boundary. This trend in oxygen isotopes is interpreted as a result of gradual warming. Latitudinal climatic zoning was probably decreasing during the Late Jurassic, with a pronounced climatic zoning close to Middle–Late Jurassic transition, and a weak climatic zoning at the J/K boundary.

Acknowledgments

This study resulted from research financed by the Czech Science Foundation within project No. 205/07/1365 “Integrated Stratigraphy and Geochemistry of the Jurassic/Cretaceous Boundary Strata in the Tethyan and Boreal Realm” and MSM0021620855, and the grant project from the Russian Foundation for Basic Researches No. 05-09-00456 and Program 24 of the Presidium of RAS. The paper benefited from the extensive reviews of G.P. Price and an anonymous reviewer.

References

Abbink, O., Targarona, J., Brinkhuis, H., Visscher, H., 2001. Late Jurassic to earliest Cretaceous palaeoclimatic evolution of the Northern Sea. Global and Planetary Change 30, 231–256.

Amodio, S., Ferreri, V., D'Argenio, B., Weissert, H., Sprovieri, M., 2008. Carbon-isotope stratigraphy and cyclostratigraphy of shallow-marine carbonates: the case of San Lorenzello, Lower Cretaceous of southern Italy. Cretaceous Research 29, 803–813.

Anderson, T.F., Arthur, M.A., 1983. Stable isotopes of oxygen and carbon and their application to sedimentologic and environmental problems. In: Arthur, M.A., Anderson, T.F., Kaplan, I.R., Veizer, J., Land, L.S. (Eds.), Stable Isotopes in Sedimentary Geology. : Short Course Notes, 10. Society of Economic Paleontologists and Mineralogists, pp. 1.1–1.151.

Anderson, T.F., Popp, B.N., Williams, A.C., Ho, L.Z., Hudson, J.D., 1994. The stable isotopic record of fossils from the Petersborough Member, Oxford Clay Formation (Jurassic), UK: palaeoenvironmental implications. Journal of Geological Society London 151, 125–138.

Barskov, I.S., Kiyashko, S.I., 2000. Thermal regime variations in the Jurassic marine basin of the East European Platform at the Callovian–Oxfordian boundary: evidence from stable isotopes in belemnite rostra. Doklady Earth Sciences 372, 643–645.

Bartolini, A., Baumgartner, P.O., Hunziker, J., 1996. Middle and Late Jurassic carbon stable-isotope stratigraphy and radiolarite sedimentation in the Umbria–Marche basin (central Italy). Eclogae Geologicae Helvetiae 89, 811–844.

Billon-Bruyat, J.P., Lecuyer, C., Martineau, F., Mazin, J.M., 2005. Oxygen isotope composition of Late Jurassic vertebrate remains from lithographic limestones of western Europe: implications for the ecology of fish, turtles, and crocodillans. Palaeogeography, Palaeoclimatology, Palaeoecology 216, 359–375.

Bodin, S., Fiet, N., Godet, A., Matera, V., Westermann, S., Clément, A., Janssen, N.M.M., Stille, P., Föllmi, K.B., 2009. Early Cretaceous (late Berriasian to early Aptian) palaeoceanographic change along the northwestern Tethyan margin (Vocontian Trough, southeastern France): $\delta^{13}C$, $\delta^{18}O$ and Sr-isotope belemnite and whole-rock records. Cretaceous Research 30, 1247–1262.

Broecker, W.S., 1989. The salinity contrast between the Atlantic and Pacific Oceans during glacial time. Paleoceanography 4, 207–212.

Chadima, M., Pruner, P., Šlechta, S., Grygar, T., Hirt, A.M., 2006. Magnetic fabric variations in Mesozoic black shales, Northern Siberia, Russia: possible paleomagnetic implications. Tectonophysics 418, 145–162.

Denison, R.E., Koepnick, R.B., Fletcher, A., Howell, M.W., Callaway, W.S., 1994. Criteria for retention of original seawater $^{87}Sr/^{86}Sr$ in ancient shelf limestones. Chemical Geology (Isotope Geoscience Section) 112, 131–143.

Dercourt, J., Gaetani, M., Vrielynck, B., Barrier, E., Biju-Duval, B., Brunet, M.F., Cadet, J.P., Crasquin, S., Sandulescu, M. (Eds), 2000. Atlas Peri-Tethys, Paleogeographical maps. CCGM/CGMW, Paris.

Ditchfield, P.W., 1997. High northern palaeolatitude Jurassic–Cretaceous palaeotemperature variation: new data from Kong Karls Land, Svalbard. Palaeogeography, Palaeoclimatology, Palaeoecology 130, 163–175.

Dromart, G., Garcia, J.-P., Picard, S., Atrops, F., Lécuyer, C., Sheppard, S.M.F., 2003. Ice age at the Middle–Late Jurassic transition? Earth and Planetary Science Letters 213, 205–220.

Dunca, E., Doguzhaeva, L., Schöne, B.R., Schootbrugge, B. van de., 2006. Growth patterns in rostra of the Middle Jurassic belemnite *Megateuthis giganteus*: controlled by the Moon? Acta Universitatis Carolinae – Geologica 49, 107–117.

Dzyuba, O., Zakharov, V.A., Košťák, M., 2007. Belemnites of the Jurassic/Cretaceous boundary interval from the Nordvik Peninsula (Northern Siberia). VI. International Symposium Cephalopods—Present and Past, September 14–16, 2007, Sapporo. Abstract Volume, pp. 94–95.

Frakes, L.A., 1979. Climates through Geologic Time. Elsevier, Amsterdam.

Gradstein, F.M., Ogg, J.G., Smith, A.G. (Eds.), 2004. A Geologic Time Scale 2004. Cambridge University Press, Cambridge, U.K.

Gröcke, D.R., Price, G.D., Ruffell, A.H., Mutterlose, J., Baraboshkin, E., 2003. Isotopic evidence for Late Jurassic–Early Cretaceous climate change. Palaeogeography, Palaeoclimatology, Palaeoecology 202, 97–118.

Hallam, A., 1993. Jurassic climates as inferred from the sedimentary and fossil record. Philosophical Transactions of the Royal Society of London, Series B 341, 287–296.

Hansen, K.W., Wallmann, K., 2003. Cretaceous and Cenozoic evolution of seawater composition, atmospheric O_2 and CO_2: a model perspective. American Journal of Science 303, 94–148.

Houša, V., Krs, M., Krsová, M., Pruner, P., 1996. Magnetostratigraphic and micropaleontological investigation along the Jurassic–Cretaceous boundary strata, Brodno near Žilina (Western Slovakia). Geologica Carpathica 47, 135–151.

Houša, V., Krs, M., Krsová, M., Man, O., Pruner, P., Venhodová, D., 1999. High-resolution magnetostratigraphy and micropaleontology across the J/K boundary strata near Žilina, western Slovakia: summary and results. Cretaceous Research 20, 699–717.

Houša, V., Krs, M., Krsová, M., Man, O., Pruner, P., Venhodová, D., Cecca, F., Nardi, G., Piscitello, M., 2004. Combined magnetostratigraphic, palaeomagnetic and calpionellid investigations across Jurassic/Cretaceous boundary strata in the Bosso Valley, Umbria, central Italy. Cretaceous Research 25, 771–785.

Houša, V., Pruner, P., Zakharov, V.A., Kostak, M., Chadima, M., Rogov, M.A., Šlechta, S., Mazuch, M., 2007. Boreal–Tethyan correlation of the Jurassic–Cretaceous boundary interval by magneto- and biostratigraphy. Stratigraphy and Geological Correlation 15, 297–309.

Houša, V., Pruner, P., Zakharov, V., Košťák, M., Chadima, M., Rogov, M., Šlechta, S., Mazuch, M., 2008. Principal results of Boreal–Tethyan correlation of the Jurassic–Cretaceous boundary by magnetostratigraphy. The 5th International Symposium of IGCP 506 on: Marine and non-marine Jurassic: global correlation and major geological events, Tunisia (Hammamet), March 28–31, 2008, Abstract Volume, pp. 81–82.

Jenkyns, H.C., 1996. Relative sea-level change and carbon isotopes: data from the Upper Jurassic (Oxfordian) of central and Southern Europe. Terra Nova 8, 75–85.

Jenkyns, H.C., Jones, C.E., Gröcke, D.R., Hesselbo, S.P., Parkinson, D.N., 2002. Chemostratigraphy of the Jurassic System: applications, limitations and implications for palaeoceanography. Journal of the Geological Society London 159, 351–378.

Kaplan, M.E., 1978. Calcite pseudomorphoses from the Jurassic and Lower Cretaceous deposits of Eastern Siberia. Soviet Geology and Geophysics 12, 62–70 (in Russian).

Kemper, E., 1987. Das Klima der Kreide-Zeit. Geologisches Jahrbuch A 96, 5–185.

Lécuyer, C., Allemand, P., 1999. Modelling of the oxygen isotope evolution of seawater: Implications for the climate interpretation of the $\delta^{18}O$ of marine sediments. Geochimica et Cosmochimica Acta 63, 351–361.

Lécuyer, C., Picard, S., Garcia, J.-P., Shepard, S.M.F., Grandjean, P., Dromart, G., 2003. Thermal evolution of Tethyan surface waters during the Middle–Late Jurassic: evidence from $\delta^{18}O$ of marine fish teeth. Paleoceanography 18, 1076.

Louis-Schmid, B., Rais, P., Bernasconi, S.M., Pellenard, P., Collin, P.-Y., Weissert, H., 2007. Detailed record of the mid-Oxfordian (Late Jurassic) positive carbon-isotope excursion in two hemipelagic sections (France and Switzerland): a plate tectonic trigger? Palaeogeography, Palaeoclimatology, Palaeoecology 248, 459–472.

McArthur, J.M., Doyle, P., Leng, M.J., Reeves, K., Williams, C.T., Gracia-Sanchez, R., Howarth, R.J., 2007a. Testing palaeo-environmental proxies in Jurassic belemnites: Mg/Ca, Sr/Ca, Na/Ca, $\delta^{18}O$ and $\delta^{13}C$. Palaeogeography, Palaeoclimatology, Palaeoecology 252, 464–480.

McArthur, J.M., Janssen, N.M.M., Reboulet, S., Leng, M.J., Thirlwall, M.F., van de Schootbrugge, B., 2007b. Palaeotemperatures, polar ice volumes, and isotope stratigraphy (Mg/Ca, $\delta^{18}O$, $\delta^{13}C$, $^{87}Sr/^{86}Sr$): the Early Cretaceous (Berriasian, Valanginian, Hauterivian). Palaeogeography, Palaeoclimatology, Palaeoecology 248, 391–430.

McArthur, J.M., Mutterlose, J., Price, G.D., Rawson, P.F., Ruffell, A., Thirlwall, M.F., 2004. Belemnites of Valanginian, Hauterivian and Barremian age: Sr-isotope stratigraphy, composition ($^{87}Sr/^{86}Sr$, $\delta^{13}C$, $\delta^{18}O$, Na, Sr, Mg), and palaeoceanography. Palaeogeography, Palaeoclimatology, Palaeoecology 202, 253–272.

Michalík, J., 2009. 3rd Workshop on the Jurassic/Cretaceous boundary of the IUGS Subcommission of Cretaceous Stratigraphy, Milano, Italy. Geologica Carpathica 60, 306.

Michalík, J., Reháková, D., Halásová, E., Lintnerová, O., 2009. The Brodno section — a potential regional stratotype of the Jurassic/Cretaceous boundary (Western Carpathians). Geologica Carpathica 60, 213–232.

Milliman, J.D., 1974. Marine Carbonates. Springer, Berlin.

Mizera, J., Řanda, Z., 2009. Neutron and photon activation analyses in geochemical characterization of sediment profiles at the Jurassic–Cretaceous boundary. Journal of Radioanalytical and Nuclear Chemistry 282, 53–57.

Nikitenko, B.I., Pestchevitskaya, E.B., Lebedeva, N.K., Ilyina, V.I., 2008. Micropaleontological and palynological analyses across the Jurassic–Cretaceous boundary on Nordvik Peninsula, Northeast Siberia. Newsletters on Stratigraphy 42, 181–222.

Nunn, E.V., Price, G.D., 2010. Late Jurassic (Kimmeridgian–Tithonian) stable isotopes ($\delta^{18}O$, $\delta^{13}C$) and Mg/Ca ratios: New palaeoclimate data from Helmsdale, northeast Scotland. Palaeogeography, Palaeoclimatology, Palaeoecology 292, 321–335.

Nunn, E.V., Price, G.D., Hart, M.B., Page, K.N., Leng, M.J., 2009. Isotopic signals from the Callovian–Kimmeridgian (Middle–Upper Jurassic) belemnites and bulk organic carbon, Staffin Bay, Isle of Skye, Scotland. Journal of the Geological Society London 166, 633–641.

Olóriz, F., Reolid, M., Rodríguez-Tovar, F.J., 2004. Microboring and taphonomy in Middle Oxfordian to lowermost Kimmeridgian (Upper Jurassic) from the Prebetic Zone (southern Iberia). Palaeogeography, Palaeoclimatology, Palaeoecology 212, 181–197.

Padden, M., Weissert, H., Funk, H., Schneider, S., Gansner, C., 2002. Late Jurassic lithological evolution and carbon isotope stratigraphy of the Western Tethys. Eclogae Geologicae Helvetiae 95, 333–346.

Podlaha, O.G., Mutterlose, J., Veizer, J., 1998. Preservation of $\delta^{18}O$ and $\delta^{13}C$ in belemnite rostra from the Jurassic/Early Cretaceous successions. American Journal of Science 298, 324–347.

Price, G.D., 1999. The evidence and implication for polar-ice during the Mesozoic. Earth Science Reviews 48, 183–210.

Price, G.D., Mutterlose, J., 2004. Isotopic signals from the late Jurassic–early Cretaceous (Volgian–Valanginian) sub-Arctic belemnites, Yatria River, Western Siberia. Journal of the Geological Society London 161, 959–968.

Price, G.D., Page, K.N., 2008. A carbon and oxygen isotopic analysis of molluscan faunas from the Callovian–Oxfordian boundary at Redcliff Point, Weymouth, Dorset: implications for belemnite behaviour. Proceedings of the Geologists' Association 119, 153–160.

Price, G.D., Rogov, M.A., 2009. An isotopic appraisal of the Late Jurassic greenhouse phase in the Russian platform. Palaeogeography, Palaeoclimatology, Palaeoecology 273, 41–49.

Price, G.D., Ruffell, A.H., Jones, C.E., Kalin, R.M., Mutterlose, J., 2000. Isotopic evidence for temperature variation during the early Cretaceous (late Ryazanian–mid Hatuerivian). Journal of Geological Society London 157, 335–343.

Price, G.D., Twitchett, R.J., Smale, C., Marks, V., 2009a. Isotopic analysis of the life history of the enigmatic squid Spirula spirula, with implications for studies of fossil cephalopods. Palaios 24, 273–279.

Price, G.D., Wilkinson, D., Hart, M.B., Page, K.N., Grimes, S.T., 2009b. Isotopic analysis of coexisting Late Jurassic fish otoliths and molluscs: implications for upper-ocean water temperature estimates. Geology 37, 215–218.

Pruner, P., Housa, V., Zakharov, V., Kostak, M., Chadima, M., Rogov, M., Slechta, S., Mazuch, M., 2007. The first Boreal–Tethyan correlation of the Jurassic–Cretaceous boundary interval by the magnetostratigraphy. Joint Asembly Supplement, abstract GP 52A-05. AGU Joint Assembly, Acapulco, Mexico: Eos Transactions American Geophysical Union, 88 (23), Joint Assembly Supplement, Abstract No. GP 52A-05.

Pruner, P., Houša, V., Olóriz, F., Košťák, M., Krs, M., Man, O., Schnabl, P., Venhodová, D., Tavera, J.M., Mazuch, M., 2010. High-resolution magnetostratigraphy and biostratigraphic zonation of the Jurassic/Cretaceous boundary strata in the Puerto Escaño section (S Spain). Cretaceous Research 31, 192–206.

Rexfort, A., Mutterlose, J., 2006. Stable isotope records from Sepia officinalis — a key to understanding the ecology of belemnites? Earth and Planetary Science Letters 247, 212–221.

Riboulleau, A., Baudin, F., Deaux, V., Hantzpergue, P., Renard, M., Zakharov, V., 1998. Évolution de la paléotempérature de eaux de la plate-forme rusee au cours du Jurassique supérieur. Comptes Rendus de l'Académie des Sciences, Série II 326, 239–246.

Rogov, M.A., Price, G.D., 2010. New stratigraphic and isotope data on the Kimmeridgian–Volgian boundary beds of the Subpolar Urals, Western Siberia. Geological Quarterly 54, 33–40.

Rogov, M.A., Zakharov, V.A., 2010. Jurassic and Lower Cretaceous glendonite occurrences and their implication for Arctic paleoclimate reconstructions and stratigraphy. Earth Science Frontiers 17, Special Issue, 345–347.

Rohling, E.J., 2007. In: Elias, S.A. (Ed.), Oxygen isotope composition of seawater. : Encyclopedia of Quaternary Science, vol. 3. Elsevier, pp. 1748–1756.

Rosales, I., Robles, S., Quesada, S., 2004. Elemental and oxygen isotope composition of Early Jurassic belemnites: salinity vs. temperature signals. Journal of Sedimentary Research 74, 342–354.

Ruffell, A.H., Price, G.D., Mutterlose, J., Kessels, K., Baraboshkin, E., Gröcke, D.R., 2002. Palaeoclimate indicators (clay minerals, calcareous nannofossils, stable isotopes) compared from two successions in the late Jurassic of the Volga Basin (SE Russia). Geological Journal 37, 17–33.

Saks, V.N., Nalnyaeva, T.I., 1979. Peculiarities of distribution of the Boreal belemnoids. In: Saks, V.N., Zakharov, V.A. (Eds.), Habitat Conditions of the Mesozoic Marine Boreal Faunas. Nauka, Novosibirsk, pp. 9–23.

Schnabl, P., Pruner, P., Houša, V., Chadima, M., Šlechta, S., 2008. Summary of basic magnetic parameters on the Jurassic–Cretaceous boundary. Contributions to Geophysics and Geodesy 38, 123–124 Special Issue.

Scotese, C.R., Golonka, J., 1992. Paleogeographic atlas. PALEOMAP Progress Report 20-0682. Department of Geology, University of Texas at Arlington.

Shackleton, N.J., Kennett, J.P., 1975. Paleotemperature history of the Cenozoic and the initiation of Antarctic glaciation: Oxygen and carbon isotope analyses in DSDP Sites 277, 279 and 281. In: Kennet, J.P., Houtz, R.E., et al. (Eds.), Initial Reports of the Deep Sea Drilling Project, 29, pp. 743–756.

Smith, A.G., Smith, D.G., Funnell, B.M., 1994. Atlas of Mesozoic and Cenozoic Coastlines. Cambridge University Press, Cambridge.

Tremolada, F., Bornemann, A., Bralower, T., Koeberl, C., van de Schootbrugge, B., 2006. Paleoceanographic changes accros the Jurassic/Cretaceous boundary: the calcareous phytoplankton response. Earth and Planetary Science Letters 241, 361–371.

Valdes, P.J., Sellwood, B.W., 1992. A palaeoclimatic model for the Kimmeridgian. Palaeogeography, Palaeoclimatology, Palaeoecology 95, 47–72.

Veizer, J., 1974. Chemical diagenesis of belemnite shells and possible consequences for palaeotemperature determination. Neues Jahrbuch für Geologie und Paläontologie 147, 91–111.

Veizer, J., Ala, D., Azmy, K., Bruckschen, P., Buhl, D., Bruhn, F., Garden, G.A.F., Diener, A., Ebneth, S., Godderis, Y., Jasper, T., Korte, G., Pawellek, F., Podlaha, O.G., Strauss, H., 1999. $^{87}Sr/^{86}Sr$, $\delta^{13}C$ and $\delta^{18}O$ evolution of Phanerozoic seawater. Chemical Geology 161, 59–88.

Veizer, J., Fritz, P., 1976. Possible control of post-depositional alteration in oxygen palaeotemperature determinations. Earth and Planetary Science Letters 33, 255–260.

Wallmann, K., 2001. Controls on the Cretaceous and Cenozoic evolution of seawater composition, atmospheric CO_2 and climate. Geochmica et Cosmochimica Acta 65, 3005–3025.

Weissert, H., Channell, J.E.T., 1989. Tethyan carbonate carbon isotope stratigraphy across the Jurassic–Cretaceous boundary: an indicator of decelerated global carbon cycling? Paleoceanography 4, 483–494.

Weissert, H., Erba, E., 2004. Volcanism, CO_2 and palaeoclimate: a Late Jurassic–Early Cretaceous carbon and oxyge isotope record. Journal of the Geological Society 161, 695–702.

Weissert, H., Lini, A., 1991. Ice age interludes during the time of Cretaceous greenhouse climate? In: Müller, D.W., McKenzie, J.A., Weissert, H. (Eds.), Controversies in Modern Geology. Academic Press, pp. 173–191.

Weissert, H., Mohr, H., 1996. Late Jurassic climate and its impact on carbon cycling. Palaeogegraphy, Palaeoecology, Palaeoclimatology 122, 27–43.

Wierzbowski, H., 2004. Carbon and oxygen isotope composition of Oxfordian—Early Kimmeridgian belemnite rostra: palaeoenvironmental implications for Late Jurassic seas. Palaeogeography, Palaeoclimatology, Palaeoecology 203, 153–168.

Wierzbowski, H., Joachimski, M.M., 2009. Stable isotopes, elemental distribution, and growth rings of belemnopsid belemnite rostra: proxies for belemnite life habitat. Palaios 25, 377–386.

Wierzbowski, H., Rogov, M.A., 2009. Oxygen and carbon isotope records of belemnite rostra from the Middle–Upper Jurassic boundary at Dubki (Saratov Volga area, Russia): preliminary results. In: Zakharov, V.A. (Ed.), Jurassic System of Russia: Problems of Stratigraphy and Paleogeography. 3rd all-Russian Meeting: Scientific Materials. Nauka, Saratov, pp. 25–28 (in Russian).

Wiese, F., Košták, M., Wood, C.J., 2009. The Upper Cretaceous belemnite *Praeactinocamax plenus* (Blainville, 1827) from Lower Saxony (Upper Cenomanian, northwest Germany) and its distribution pattern in Europe. Paläontologische Zeitschrift 83, 309–321.

Wimbledon, W.A.P., 2008. The Jurassic–Cretaceous boundary. An age-old correlative enigma. Episodes 31, 423–428.

Zakharov, V.A., Baudin, F., Dzyuba, O.S., Daux, V., Zverev, V.V., Renard, M., 2005. Isotopic and faunal record of high paleotemperatures in the Kimmeridgian of the Subpolar Urals. Russian Geology and Geophysics 46, 1–19.

Zakharov, V.A., Rogov, M.A., 2008a. Let Volgian stage stay in the Jurassic. Russian Geology and Geophysics 49, 408–412.

Zakharov, V.A., Rogov, M.A., 2008b. The Upper Volgian Substage in Northeast Siberia (Nordvik Peninsula) and its panboreal correlation based on ammonites. Stratigraphy and Geological Correlation 16, 81–94.

Zakharov, Y.D., Smyshlyaeva, O.P., Shigeta, Y., Popov, A.M., Zonova, T.D., 2006. New data on isotopic composition of Jurassic–Early Cretaceous cephalopods. Progress in Natural Science 16, 50–67 (Special Issue SI).